

© К. Zabolotnyi<sup>1</sup>, А. Burkov<sup>1</sup>, О. Panchenko<sup>1</sup>,  
О. Zhupiiiev<sup>1</sup>, V. Symonenko<sup>1</sup>

<sup>1</sup> Dnipro University of Technology, Dnipro, Ukraine

## OPTIMIZATION OF CONTACT STRESSES IN SHOE BRAKES OF MINE HOISTING MACHINES

© К.С. Заболотний<sup>1</sup>, А.О. Бурков<sup>1</sup>, О.В. Панченко<sup>1</sup>,  
О.Л. Жупієв<sup>1</sup>, В.В. Симоненко<sup>1</sup>

<sup>1</sup>Національний технічний університет «Дніпровська політехніка», Дніпро, Україна

## ОПТИМІЗАЦІЯ КОНТАКТНИХ НАПРУЖЕНЬ У КОЛОДОЧНИХ ГАЛЬМАХ ШАХТНИХ ПІДЙОМНИХ МАШИН

**Purpose.** The research aims to develop recommendations for reducing the maximum contact stresses between the brake lining and the mine hoisting machine drum.

**Methods.** Existing methodologies for calculating shoe brakes of mine hoisting machines often use a hypothesis that assumes absolute stiffness of the brake rim and beam. The developed methodology, using a set of various mathematical and engineering methods, makes it possible to determine the pattern of contact pressure distribution depending on the ratio of the brake lining transverse stiffness to the brake beam bending stiffness.

**Findings.** An analytical model of the brake beam, presented in the form of a circular bar of constant section, has been developed, which is based on the Winkler elastic foundation concept, providing the ability to adapt the stiffness in accordance with the complex brake lining parameters. The stress-strain analysis has identified a key dimensionless indicator – the relative lining stiffness, which has a significant impact on the contact pressure distribution.

The research results are presented in the form of a comparative analysis of various design approaches used to provide a more uniform contact pressure distribution along the brake beam.

**Originality.** The proposed analytical model is based on the Winkler elastic foundation involving variable stiffness parameters, which provides high accuracy in modeling the actual physical characteristics of the braking system. This is far superior to traditional methodologies that are based on the assumption of absolute component stiffness, thereby increasing the relevance and scientific value of the results.

**Practical implications.** The proposed recommendations make it possible to optimize the design of braking systems, reducing maximum contact stresses, thereby improving the efficiency, reliability and durability of mine hoisting machines.

**Keywords:** *braking system, mine hoisting machine, contact stresses, Winkler elastic foundation, relative stiffness, analytical model, braking system optimization, finite element method, SolidWorks Simulation.*

**Introduction.** Increasing mining volumes require increasing the efficiency and reliability of mine hoisting machines (MHM). It is known that the primary means of protecting a hoisting plant from an accident is its braking system [1–3]. The actual technical problem is to reduce the contact pressure of MHM shoe brakes, for the solution of which it is necessary to study the influence of the brake beam (below referred to as beam)

parameters on the pattern of contact pressure distribution and to create a refined methodology for the development of MHM braking systems [4–6].

The papers [1, 2] present an improved mathematical model of brake shoe and track system for drum brakes. The model makes it possible to calculate such brake characteristics as braking coefficient, pressure distribution between the brake shoe and track, as well as the braking torque, given the elastic properties of the brake components and the initial contact geometry between them. The research methodology differs from the traditional ones, which ignore elastic deformation and real contact geometry.

Scientific results show that the new model provides more accurate prediction of braking system performance than existing methods, as confirmed by full-scale tests and measurements. Special attention is paid to pressure distribution and braking track movements.

While the paper provides an important contribution to understanding of braking system dynamics, there are some disadvantages that may affect the overall perception of its results. The paper states that the disagreement between theoretical predictions and real measurements may be caused by errors in the measurement of components or their assembly, but there is no clear strategy for addressing these differences in the model. Although the paper proposes one model, it makes no comparison with other potential approaches or models that could be used to analyze such systems, limiting the reader's ability to assess the proposed model relative effectiveness.

The study [3] presents a parametric modeling of a drum brake using 3D finite element methods (FEM) to analyze non-contact interaction. The study is relevant due to the need to improve the performance of drum brakes in automobiles, focusing on the aspects of interface stiffness, friction coefficient and line pressure. The methodology is based on the use of FEM for modal analysis of a drum brake to obtain its eigenfrequencies and to study the system instability. The main scientific results include the effectiveness of using an asymmetric computational solution for linear system behavior converted from non-linear contact behavior. Based on the presented paper [3], the following disadvantages can be identified. The paper focuses on theoretical modeling and analysis, but does not provide enough data on experimental testing of theoretical models. Lack of detailed experimental data or comparison with real measurements may raise questions about the practical suitability of the obtained results. The paper does not discuss the stability and reliability of the proposed model during long-term operation, which is an important aspect for braking systems used in the automotive industry.

**Problem statement.** Many well-known scientists, namely B.L. Davydov, Z.M. Fedorova, N.S. Karpyshev, V.I. Belobrov, V.F. Abramovskyi, V.I. Samusya and V.I. Vasiliev, Z. Barecki, S.F. Scieszka, participated in the development of braking devices for mine hoisting machines. The basic methodology for calculating the braking devices of a mine hoisting machine is described in the works of B.L. Davydov, Z.M. Fedorova, N.S. Karpishev. This methodology is based on the hypothesis that the brake rim and beam are assumed to be absolutely stiff. In subsequent numerous works on improvement of brake calculation methodology, dynamic and thermal processes occurring in the braking system components were taken into account. Thus, in the works of V.I. Belobrov, V.I. Samusya, V.F. Abramovskyi and V.I. Vasiliev, the issues of the hoisting plant

dynamics at operating and emergency braking modes are considered. Most importantly, the stiffness of the brake rim and beam has not been substantiated.

The results of calculating the stress-strain state for mine hoisting machine brakes have some discrepancies with those described in the literature. For example, the pattern of the contact pressure distribution along the brake beam is not sinusoidal with peak values in the center of the shoe. On the contrary, it has a distinct edge effect, the so-called U-shaped nature. Therefore, an urgent scientific task is to determine the factors influencing the contact pressure distribution and determine the scope of the hypothesis application of an absolutely stiff beam.

**Main part of the research.** A brake shoe model has been constructed to study the impact of the factors [4, 5] – a constant cross-section circular beam on an elastic base, loaded by two horizontal forces (Fig. 1). The following indications are used in this figure:  $h$  – is the lining thickness;  $N$  – is the braking force acting on the shoe;  $R$  – a brake rim radius;  $\gamma$  – is the contact arc half;  $\varphi$  – is the current angular coordinate.

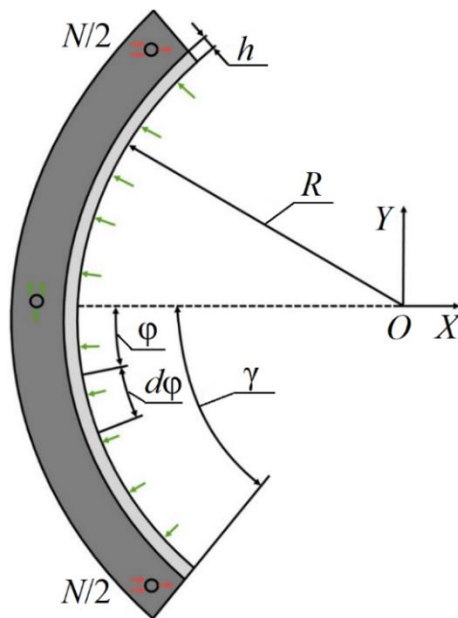


Fig. 1. Brake shoe computation model

Figure 1 shows a scheme of a brake beam in the form of a circle segment with a radius  $R$ , which is under the action of horizontal forces  $N/2$  applied at the edges. These forces are constituents of the total force  $N$ , acting perpendicular to the figure plane and distributed tangentially to the inner surface of the beam, simulating the braking mechanism action. The  $OXY$  coordinate system is centered at point  $O$ , which is the beam segment curvature center. The angle  $\gamma$  determines the sector within which the specified uniformly distributed force is applied. The radial lines emanating from point  $O$  show the directions of the distributed forces along the tangent forming the torque relative to center  $O$ . The force vectors act in the direction opposite to the torque induced by the tractive forces in the mining machine, the model of which is under study. Mark  $d\varphi$  indicates the angle-differential element on which the distributed force is applied, that is, the small beam sector where the force acts.

The  $\pm N/2$  marks in the upper and lower parts of the figure indicate the points of applied external forces. These forces generate contact pressure between the beam and the brake lining and are critical to beam strength and durability calculations.

Calculations according to N.S. Karpyshev's methodology are based on the following formulas:

$$M_T = \frac{3PR}{n}; p_{\max} = \frac{M_T}{2fBR^2 \sin \gamma}; N = p_{\max}BR(\gamma + 0,5 \sin \gamma),$$

where  $M_T$  – is the braking torque;  $p_{\max}$  – is the maximum contact pressure.

For example, consider the brake shoe of the mine hoisting machine of CR-5×3.2/0.85 type with the following parameters:  $R = 2480$  mm;  $B = 400$  mm – is the brake rim width;  $\gamma = 50^\circ$ ;  $H = 400$  mm – is the brake beam height;  $h = 80$  mm;  $E = 2.1 \times 10^{11}$  Pa – is the beam material elasticity modulus;  $E_l = 3 \times 10^8$  Pa – is the lining press material elasticity modulus 143 – 63;  $P = 2.06 \times 10^5$  N – is the difference in the static cable tensions;  $n = 2$  – is the number of brake beams;  $f = 0.3$  – is the friction coefficient.

Results of calculations based on these formulas are as follows:  $M_T = 772$  kN · m;  $p_{\max} = 0.68$  MPa;  $N = 924.8$  kN,

The following boundary conditions are used for modeling:

- horizontal forces  $N/2$  are applied to the axles at the edges of the brake beam;
- the lining is fixed against movements in the radial direction;
- the central beam axis is fixed against movements in the vertical direction.

An analytical solution to this problem was obtained from the study of the bicycle wheel strength by F.V. Feodosiev and A.H. Zhukovsky.

When developing the mathematical model, equilibrium equations play a key role in determining the dynamic properties of the system. The equations are as follows:

$$\frac{dT}{d\varphi} + Q + \tau R = 0; \tag{1}$$

$$\frac{dQ}{d\varphi} - T - qR = 0; \tag{2}$$

$$\frac{dM}{d\varphi} + QR = 0, \tag{2}$$

where  $T$  – is the longitudinal force in the beam;  $Q$  – is a shearing force;  $M$  – is a bending moment;  $q$  – is distributed contact force;  $\tau$  – is distributed friction force.

The distributed contact force is determined as:

$$q = -kw, \tag{4}$$

where  $w$  – is the beam deflection;  $k$  – is the transverse lining stiffness.

$$k = E_{\mu}B / h, \tag{5}$$

where  $E_{\mu}$  – is the lining material elasticity modulus.

The equation for the distributed friction force has the following form:

$$\tau = fkw \quad (6)$$

Hooke's law for the torque in a beam is formulated as:

$$M = -\frac{EI}{R} \frac{d\theta}{d\varphi}, \quad (7)$$

where  $E$  – is the beam material elasticity modulus;  $I$  – is the beam section inertia moment.

Kinematic dependence is specified as:

$$\theta = \frac{1}{R} \left( \frac{dw}{d\varphi} + v \right), \quad (8)$$

where  $v$  – is the tangential displacement.

The inextensibility condition is determined as follows:

$$w = dv / d\varphi. \quad (9)$$

By substituting expressions (4-9) into equation (1-3), we have:

$$\begin{aligned} & \frac{EI}{R^3} \left( \frac{d^5 w}{d\varphi^5} + \frac{d^3 w}{d\varphi^3} \right) + kR \frac{dw}{d\varphi} + \frac{EI}{R^3} \left( \frac{d^3 w}{d\varphi^3} + \frac{dw}{d\varphi} \right) + fkRw = \\ & = \frac{EI}{R^3} \left( \frac{d^6 v}{d\varphi^6} + \frac{d^4 v}{d\varphi^4} \right) + kR \frac{d^2 v}{d\varphi^2} + \frac{EI}{R^3} \left( \frac{d^4 v}{d\varphi^4} + \frac{d^2 v}{d\varphi^2} \right) + fkR \frac{dv}{d\varphi} = 0. \end{aligned} \quad (10)$$

Equation (10) is a complex dependence that includes both physical and geometric parameters of the system, allowing a detailed analysis of the stress distribution in the beam and lining.

Determine the relative stiffness  $\lambda$  as the ratio of the transverse lining stiffness to the bending stiffness of the beam:

$$\lambda = E_l B R^4 / hEI,$$

where  $E_l$  – is the lining material elasticity modulus,  $B$  – is the lining width,  $R$  – is the beam radius,  $h$  – is the lining thickness,  $E$  – is the beam material elasticity modulus,  $I$  – is the beam section inertia moment.

Accordingly, the equation (10) takes the following form:

$$\frac{d^6 v}{d\varphi^6} + 2 \frac{d^4 v}{d\varphi^4} + (1 + \lambda) \frac{d^2 v}{d\varphi^2} + f\lambda \frac{dv}{d\varphi} = 0.$$

Its characteristic equation is:

$$n \left( n^5 + 2n^3 + (1 + \lambda)n + f\lambda \right) = 0.$$

Since the influence of friction is insignificant, we ignore it.

By substituting  $n^2 = m$ , we have

$$m(m^2 + 2m + 1 + \lambda) = 0.$$

For the studied machine, the following roots of this equation can be obtained:

$$m = \begin{cases} 0; \\ -1 + \sqrt{-\lambda} = -1 + i \cdot 12,3; \\ -1 - \sqrt{-\lambda} = -1 - i \cdot 12,3. \end{cases}$$

Hence,  $n$  is:

$$n = \begin{cases} 0 \\ 0 \\ 2,35 + 2,56i \\ -2,35 - 2,56i \\ 2,35 - 2,56i \\ -2,35 + 2,56i \end{cases}$$

Force boundary conditions:

$$M(\gamma) = 0; \quad Q(\lambda) = \frac{-N}{2} \cos \gamma; \quad T(\lambda) = \frac{N}{2} \sin \gamma.$$

Finally, the contact pressure distribution formula along the lining has the form:

$$q(\lambda, \varphi) = k (C_0 + \text{sh}(\alpha\varphi) \sin \beta\varphi (\beta C_1 - \alpha C_2) + \text{ch}(\alpha\varphi) \cos \beta\varphi (\alpha C_1 + \beta C_2)) / B, \quad (11)$$

where  $C_0 = \sqrt{\lambda} (\text{ch}(\alpha\gamma) \cos \beta\gamma (\beta C_1 - \alpha C_2) + \text{sh}(\alpha\gamma) \sin \beta\gamma (\alpha C_1 + \beta C_2))$ .

Other coefficients are determined as follows:

$$C_1 = \frac{B_1 A_{22} - B_2 A_{12}}{B_0}; \quad C_2 = \frac{B_2 A_{11} - B_1 A_{21}}{B_0}; \quad B_0 = A_{11} A_{22} - A_{12} A_{21};$$

$$B_1 = \frac{N}{2kR} \sin \gamma; \quad B_2 = \frac{-NR^3}{2\sqrt{\lambda} EI} \cos \gamma.$$

Coefficients  $A_{11}$ ,  $A_{12}$ ,  $A_{21}$ ,  $A_{22}$  depend on  $\alpha$ ,  $\beta$ ,  $\varphi$ ,  $\gamma$ :

$$A_{11} = \beta \text{sh}(\alpha\varphi) \cos \beta\varphi + \alpha \text{ch}(\alpha\varphi) \sin \beta\varphi; \quad A_{12} = -\alpha \text{sh}(\alpha\varphi) \cos \beta\varphi + \beta \text{ch}(\alpha\varphi) \sin \beta\varphi;$$

$$A_{21} = -\sqrt{\lambda} \text{sh}(\alpha\gamma) \cos \beta\gamma + \text{ch}(\alpha\gamma) \sin \beta\gamma; \quad A_{22} = -\text{sh}(\alpha\gamma) \cos \beta\gamma - \sqrt{\lambda} \text{ch}(\alpha\gamma) \sin \beta\gamma;$$

$$\alpha = \sqrt{0,5(-1 + \sqrt{1 + \lambda})}; \quad \beta = \sqrt{0,5(1 + \sqrt{1 + \lambda})}.$$

Introduce the notion of relative pressure  $\chi(\lambda, \varphi)$  as the ratio of contact pressure to the pressure caused by the same force  $N$  acting on an absolutely stiff part of the same area  $F = B \cdot R \cdot 2 \cdot \gamma$ .

Plot the dependency graph of  $\chi(\lambda, \varphi)$  distribution on the relative stiffness  $\lambda$  (Fig. 2). This graph illustrates how the relative stiffness of a structure affects the contact pressure distribution pattern in a braking system.

The solid line corresponds to the value of  $\lambda = 1$  and shows a relatively flat and symmetrical pressure distribution relative to the axis  $\varphi = 0$ . Dashed line  $\lambda = 10$  already has a more distinct curvature, with peak pressure values located closer to the center ( $\varphi = 0$ ). The dot-and-dash line for  $\lambda = 100$  shows even greater curvature with a higher peak in the center. The dotted line for  $\lambda = 1000$  shows even greater centralized peak pressure, which is most different from the other curves.

As  $\lambda$  increases, that is, when the lining transverse stiffness is much higher than the beam bending stiffness, the peak of contact pressure is concentrated in the central part of the beam, which can lead to local overloading and consequently to material fatigue. In actual conditions, this may indicate a need to strengthen the central beam part or optimize the brake lining to achieve a more uniform pressure distribution.

Analyzing the above graph, it should be noted that the nature of  $\chi(\lambda, \varphi)$  distribution can be roughly divided into two main types. The maximum values of  $\chi(\lambda, \varphi)$  occur at the brake beam edges, indicating local stresses in these areas that may be critical for material fatigue and its durability. The  $\chi(\lambda, \varphi)$  distribution is sinusoidal in nature with a peak in the brake beam center, indicating a greater stress state uniformity in the middle beam part. From this it follows that there is an optimal relative stiffness value at which the values of  $\chi(\lambda, \varphi)$  at the edges and in the middle of the brake beam are equalized. Plot the dependency graph of  $\chi(\lambda, \varphi)$  at the edges and in the middle of the brake beam on the relative stiffness (Fig. 3).

This approach not only clarifies the relative stiffness critical values, but also provides an opportunity to develop improved design solutions to increase the efficiency of braking systems, reducing material fatigue and increasing the brake beam durability.

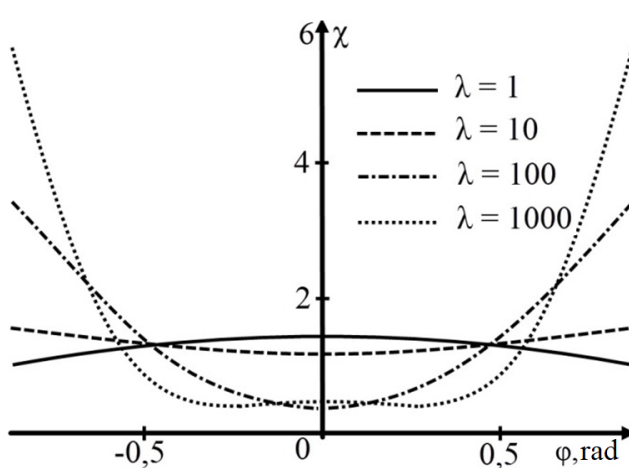


Fig. 2. Dependence of reduced pressure distribution on relative stiffness  $\lambda$

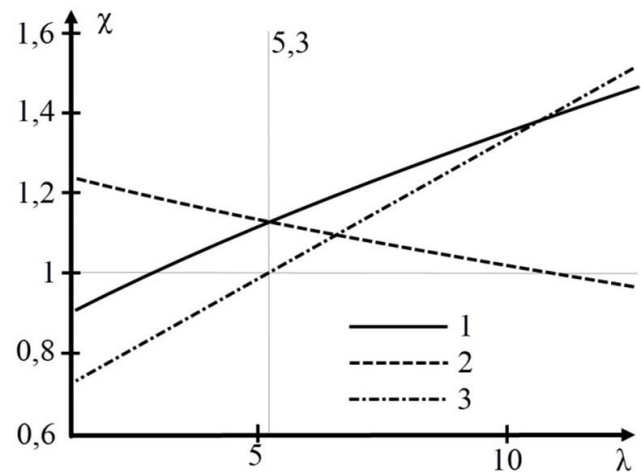


Fig. 3. Dependence of reduced pressure on relative stiffness  $\lambda$

The graph shows three curves, each representing a different aspect of the pressure distribution. Curve 1 (solid line) shows the change in  $\chi(\lambda, \varphi)$  at the brake beam edge. Curve 2 (dotted line) represents the change in  $\chi(\lambda, \varphi)$  in the middle of the beam. Curve

3 (dot-and-dash line) represents the ratio of  $\chi(\lambda, \varphi)$  at the edge to the pressure in the middle of the beam. As the relative stiffness  $\lambda$  increases,  $\chi(\lambda, \varphi)$  at the edge of the beam increases, while it decreases or remains relatively stable in the middle of the beam. The ratio of pressure at the edge to the pressure in the middle (curve 3) shows that at low values of  $\lambda$ , the pressure at the edges is lower than in the middle, but as  $\lambda$  increases, the situation changes – the pressure at the edges becomes higher. The vertical line, numbered 5.3, indicates the theoretically optimal value of  $\lambda$ , at which  $\chi(\lambda, \varphi)$  is expected to be the same at the edges and in the middle of the beam, that is, the desired pressure distribution uniformity is achieved.

This analysis can be used to design braking systems to provide a more uniform pressure distribution along the beam, which can improve system performance and reduce the risk of premature wear or damage due to non-uniform loading. For a given machine, calculated using an analytical model:

$$M_T = fR^2 \int_{-\gamma}^{\gamma} q(\varphi) d\varphi = 772 \text{ kN} \cdot \text{m}; \quad p(\varphi) = \frac{q(\varphi)}{B},$$

the maximum  $p$  is achieved with angle equal to  $\gamma$  and is 1.58 Mpa

$$N_x = R \int_{-\gamma}^{\gamma} q(\varphi) \cos \varphi d\varphi = 829 \text{ kN}.$$

Figure 4 presents two curves comparing the contact pressure distribution in the braking system. Curve 1 (solid line) shows the contact pressure distribution according to N.S. Karpyshev's model. Curve 2 (dotted line) shows the contact pressure distribution according to the developed analytical model. According to N.S. Karpyshev's model, the contact pressure has lower values compared to the analytical model, which may indicate a potential underestimation of the risk of fatigue failure of the braking system material when it is used. The analytical model shows a higher contact pressure in the central part of the brake beam, which may indicate a more realistic load distribution in real-life operating conditions. The comparison shows that the analytical model can be more accurate in predicting the pressure distribution, and therefore may be a better choice for determining the required strength and durability of brake beams. It is noted that N.S. Karpyshev's model assumes 10.3 % higher horizontal forces and 2.32 times lower contact pressures than the analytical model, which may be inadequate for high safety and reliability requirements of braking systems. This graph is therefore an important tool for choosing between theoretical models and for making adjustments in the design and operation of braking systems to minimize the risk of material fatigue and improve equipment reliability.

Figure 5 shows three curves that illustrate  $\chi(\lambda, \varphi)$  distribution from  $\varphi$ .

Curve 1 (solid line) shows the results of the analytical solution for the relative stiffness  $\lambda = 5.3$ . Curve 2 (dotted line) shows the results of a computational experiment for the same relative stiffness  $\lambda = 5.3$ . Curve 3 (dot-and-dash line) represents the computational experiment results for  $\lambda = 3.5$ .



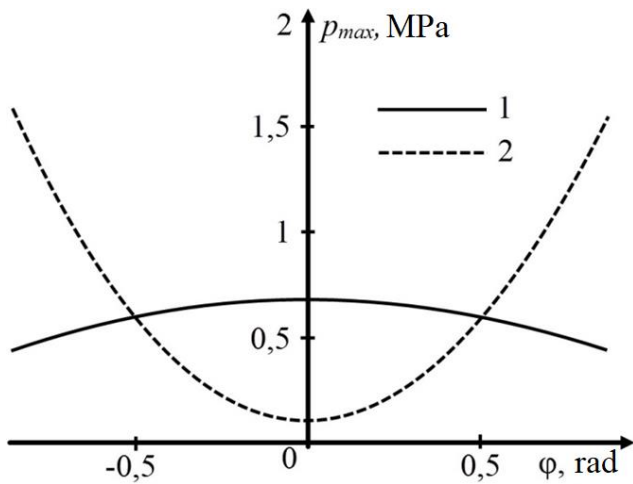


Fig. 4. Contact pressure distribution

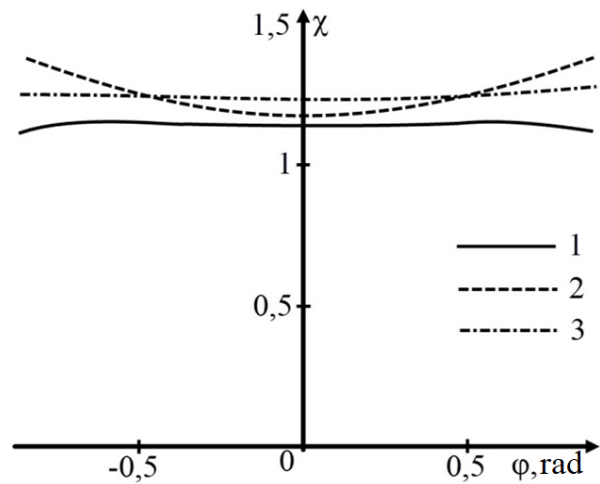


Fig. 5. Comparison of the results of an analytical solution and a computational experiment

The following conclusions can be drawn from the analysis of the graph: the analytical solution and the computational experiment at  $\lambda = 5.3$  show a difference in the pressure distribution, but maintain the general distribution trend; the pressure distribution for both methods becomes maximum in the middle of the  $\phi$  range and decreases as it approaches the edges; when the relative stiffness decreases to  $\lambda = 3.5$  (curve 3), a more uniform pressure distribution with less distinct pressure peaks is observed, indicating a reduction in local overloads.

The difference in the results of the analytical solution and the computational experiment does not exceed 33 %, which indicates a sufficient similarity of the methodologies and their suitability for engineering calculations. These results can be important in the design and optimization of braking systems, where it is necessary to achieve a uniform pressure distribution to reduce the probability of fatigue material failure and increase the brake beam durability.

The results obtained make it possible to formulate a methodology for developing a brake shoe design with the most uniform distribution of contact stresses, including the following steps:

1. Performing a computational experiment using SolidWorks Simulation program for a beam of a real structure, while determining deflections and contact pressures.
2. Determining, based on graph 3, the appropriate optimal relative stiffness value and coefficient  $j$  of change in this parameter to achieve uniform pressure distribution.
3. Reducing the lining material elasticity modulus by  $j$  times.
4. Determining the appropriate contact pressure distribution by means of a computational experiment.
5. If necessary, adjusting the coefficient  $j$  value using the iterative method to equalize the contact pressure and deflection values.
6. Development of a brake shoe design providing the obtained relative stiffness value.

7. Testing the pressure distribution for the developed brake shoe design using a computational experiment in SolidWorks Simulation.

This approach will optimize the brake shoe design, which will improve the braking system efficiency and help reduce material fatigue, extending the service life of the equipment.

Figure 6 illustrates the contact pressure distribution for various parameters of the material elasticity modulus and the relative stiffness of the beam: curve 1 (solid line) corresponds to a real structure beam with material elasticity modulus  $E_l = 300$  MPa and relative stiffness  $\lambda = 149$ ; curve 2 (dotted line) represents the real structure beam with material elasticity modulus  $E_l = 10.65$  MPa and relative stiffness  $\lambda = 7.74$ ; curve 3 (dot-and-dash line) shows a real structure beam with material elasticity modulus  $E_l = 7.29$  MPa and relative stiffness  $\lambda = 5.83$ .

Analyzing the given curves, the following conclusions can be drawn. As the material elasticity modulus and the beam relative stiffness increase, the uniformity of contact pressure distribution decreases, resulting in increased peak pressures at the edges. Curve 1 shows a significant non-uniform distribution with a high pressure concentration at the edges, which may indicate a risk of local material overloads and fatigue. Curves 2 and 3 illustrate a reduction in the difference between peak and average pressure values, which promotes a more uniform distribution and potentially increases beam durability. Reducing the material elasticity modulus by 28 times makes it possible to achieve a contact pressures distribution with a deviation from uniform of no more than 5 %, indicating the effectiveness of this method in optimizing the brake shoe properties.

Given the results of this experiment, it can be concluded that it is advisable to adapt the brake shoe material properties to achieve optimal relative stiffness and improve the braking system efficiency. There are two fundamentally different approaches to constructively achieving relative stiffness reduction. The first is to increase the beam bending stiffness, which can be achieved by increasing the brake beam thickness at its edges and using radial stiffeners on the sides. The second method is to reduce the transverse stiffness of the lining, which can be achieved by inserting a spacer gasket of flexible material between the beam and the lining.

In the context of these strategies, a series of computational experiments have been conducted to optimize the beam thickness [6]. As a result, the brake beam design for the mine hoisting machine of CR-5×3.2/0.85 type (Fig. 7, *a*) has been modified as follows (Fig. 7, *b*). Radial stiffeners in the form of 20 mm thick transverse stiffening ribs were applied. Thus, the thickness of the beam at the edges has been increased by 1.5 times compared to the middle. A layer of rubber, the thickness of which corresponds to the thickness of the lining, was added between the beam and the press material lining.

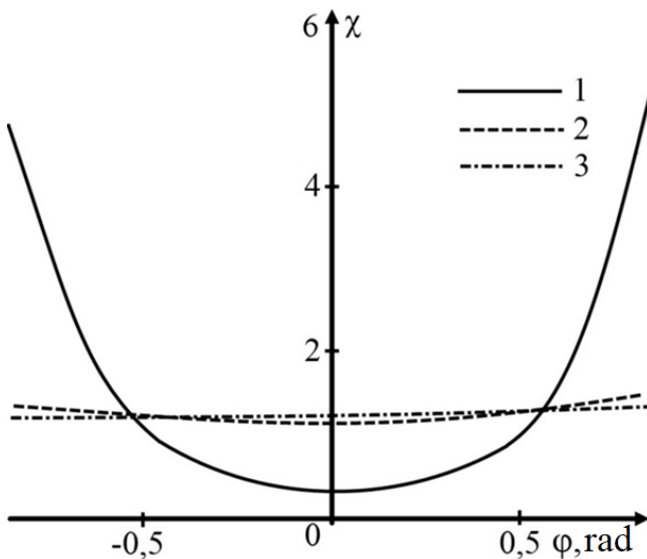


Fig. 6. Computational experiment results

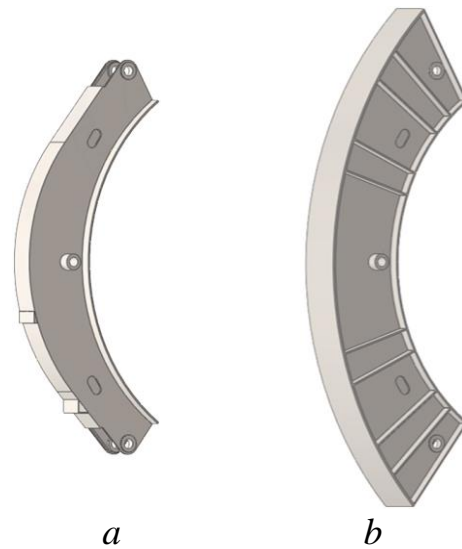


Fig. 7. Design solution to increase bending stiffness of the real structure beam

The addition of radial stiffeners has no significant effect on the contact pressure distribution and is not in itself appropriate. Adding a rubber spacer gasket, the thickness of which is commensurate with the lining thickness reduces the coefficient  $\lambda$  by more than half and is the most effective method for reducing contact pressures.

The research has revealed that the introduction of radial stiffeners does not significantly affect the contact pressure distribution and may not be considered appropriate in this context. Instead, using the rubber spacer gasket, the thickness of which corresponds to the lining thickness, reduces the  $\lambda$  coefficient by more than half, which is the most effective way to reduce contact pressures.

The table presents the results of modeling the design solutions to reduce the relative stiffness.

Table

Results of modeling the design solution

Model	Maximum contact pressure $p_{max}$ , MPa	Ratio of contact pressure values at the edge of the beam to values in the middle of the beam	Beam mass, ton
Real structure	3.45	14.71	1.71
Radial stiffening	3.06	12.82	2.23
Increasing the beam thickness	2.39	11.17	2.38
Adding a layer of rubber between the beam and the lining	2.02	6.75	1.71
All of the above mentioned	1.40	2.93	2.98

The results show a significant reduction in the maximum contact pressure and an optimization of the contact pressure ratio, indicating the success of the chosen beam design modification methods.

The research has revealed that the introduction of radial stiffeners does not have a significant effect on the contact pressure distribution and cannot be considered appropriate in this context. Instead, using the rubber spacer gasket, the thickness of which corresponds to the lining thickness, reduces the  $\chi(\lambda, \varphi)$  coefficient by more than half, which is the most effective method for reducing contact pressures.

### Conclusions.

1. The characteristic of contact pressure distribution  $\chi(\lambda, \varphi)$  correlates with the relative stiffness value  $\lambda$  and tends to change from sinusoidal to a U-shaped.

2. It has been determined that for a mine hoisting machine of CR-5×3.2/0.85 type, the contact pressure distribution along the brake beam has a U-shaped configuration, while calculations using N.S. Karpyshev's methodology indicate a sinusoidal character, which underestimates the maximum contact pressures for this machine by 2.32 times.

3. Sinusoidal law of contact pressure distribution is typical for braking devices with a relative stiffness value of less than 1.45.

4. A technology has been developed to achieve a uniform contact pressure distribution between the brake disc and lining, the main stages of which are:

- conducting a computational experiment using SolidWorks Simulation software for a beam of a real structure with determination of deflections and contact pressures;
- determining the optimal relative stiffness value and coefficient  $j$  in order to implement a uniform pressure distribution;
- reducing the lining material elasticity modulus by  $j$  times;
- determination of the appropriate contact pressure distribution by means of a computational experiment;
- refining the coefficient  $j$  value using the iterative method;
- development of a brake shoe design providing the obtained relative stiffness value.

5. To reduce the relative stiffness  $\lambda$ , it is more effective to use a spacer gasket made of flexible material, the thickness of which is equivalent to that of the lining than to change the shape of the beam.

6. The existing methodology for calculating shoe brakes, assuming the hypothesis of absolute brake beam stiffness and described in the works of B.L. Davydov, N.S. Karpyshev and Z.M. Fedorova, underestimates the values of maximum contact pressures by 2.32 times.

7. Application of the recommendations developed by the authors will reduce the maximum contact pressure in shoe brakes of mine hoisting machines.

### References

1. Barecki, Z., Scieszka, S.F. (1987). A Mathematical Model of the Brake Shoe and the Brake Path System. *N&O Joernal*, 13–17.

2. Barecki, Z., & Scieszka, S.F. (1989). Some Factors Influencing Friction Brake Performance: Part 2-A Mathematical Model of the Brake Shoe and the Brake Path System. *Journal of Mechanisms Transmissions and Automation in Design*, 111(1), 8–12. <https://doi.org/10.1115/1.3258977>
3. Ahmed, I., Fatouh, Y., & Aly, W. (2014). A parametric FE modeling of brake for non-linear analysis. *International Energy & Environment Foundation*, 5(1) 97–110.
4. Zabolotnyi, K., Zhupiiiev, O., & Molodchenko, A. (2017). Development of a model of contact shoe brake-drum interaction in the context of a mine hoisting machine. *Mining of Mineral Deposits*, 11(4), 38–45. <https://doi.org/10.15407/mining11.04.038>.
5. Zabolotnyi, K., Zhupiiiev, O., & Molodchenko, A. (2018). Development of a three-parameter model of the shoe brake contact interaction with the drum in mine hoisting machine. *E3S Web of Conferences*, 60, 00039 <https://doi.org/10.1051/e3sconf/20186000039>
6. Zabolotny, K., Zhupiev, O., & Molodchenko, A. (2015). Analysis of current trends development of mining hoist design engineering. *New Developments in Mining Engineering 2015. Theoretical and Practical Solutions of Mineral Resources Mining*. 175–179.

#### АНОТАЦІЯ

**Метою** роботи є розробка рекомендацій для зниження максимальних контактних напружень між гальмівною накладкою та барабаном шахтної підйимальної машини.

**Методика.** Існуючі методики розрахунку колодкових гальм шахтних підйимальних машин часто використовують гіпотезу, яка припускає абсолютну жорсткість гальмівного обода та гальмівної балки. Розроблена методика, яка використовує комплекс різноманітних математичних та інженерних методів, дозволяє визначити характер розподілу контактних тисків, залежно від співвідношення поперечної жорсткості гальмівної накладки до згинальної жорсткості гальмівної балки.

**Результати.** Розроблено аналітичну модель гальмівної балки, представлену у вигляді кругового бруса постійного перерізу, яка ґрунтується на концепції Вінклерівського основи, забезпечуючи можливість адаптації жорсткості відповідно до параметрів складної гальмівної накладки. Аналіз напружено-деформованого стану дозволив ідентифікувати ключовий безрозмірний показник – відносну жорсткість накладки, яка суттєво впливає на розподіл контактного тиску. Результати досліджень представлені у формі порівняльного аналізу різних конструктивних підходів, що використовуються для забезпечення більш рівномірного розподілу контактного тиску вздовж гальмівної балки.

**Наукова новизна.** Запропонована аналітична модель базується на Вінклерівській основі із залученням параметрів змінної жорсткості, що забезпечує високу точність моделювання реальних фізичних характеристик гальмівної системи. Це значно перевершує традиційні методології, котрі опираються на припущення про абсолютну жорсткість компонентів, тим самим підвищуючи релевантність і наукову цінність результатів.

**Практична цінність.** Запропоновані рекомендації дозволяють оптимізувати конструкцію гальмівних систем, знижуючи максимальні контактні напруження, що сприяє підвищенню ефективності, надійності та довговічності шахтних підйимальних машин.

**Ключові слова:** гальмівна система, шахтна підйимальна машина, контактні напруження, Вінклерівське основування, відносна жорсткість, аналітична модель, оптимізація гальмівних систем, метод кінцевих елементів, SolidWorks Simulation.